PROCEEDINGS OF SCIENCE

Energy Scan Results at Belle

Junhao Yin for the Belle Collaboration[*†]
Institute of High Energy Physics, CAS, 19B Yuquan Road, Shijingshan District, Beijing, China
E-mail: yinjh@ihep.ac.cn

In this report, we present the most recent results on the measurement on the cross sections of $e^+e^- \to \pi^+\pi^-\Upsilon(nS),\ (n=1,2,3)$, $e^+e^- \to \pi^+\pi^- h_b(1,\ 2P)$, $e^+e^- \to B_s^{(*)}\bar{B}_s^{(*)}$, and $e^+e^- \to \pi^+\pi^-\pi^0\chi_{bJ}$ $(J=0,\ 1,\ 2)$ based on energy scan data. Further analysis are also discussed.

XVII International Conference on Hadron Spectroscopy and Structure - Hadron2017
25-29 September, 2017
University of Salamanca, Salamanca, Spain

*Speaker.

†This work is supported in part by National Natural Science Foundation of China (NSFC) under contract Nos. 11475187 and 11521505; Key Research Program of Frontier Sciences, CAS, Grant No. QYZDJ-SSW-SLH011; and the CAS center for Excellence in Particle Physics (CCEPP).

PoS(Hadron2017)037

1. Introduction

As an effective theory, the potential model works well in describing the heavy quarkonia states. However, for the bottomnium beyond the B_sB_s threshold, some problems occurred. The $\Upsilon(10860)$ state, which is historically called $\Upsilon(5S)$, has unexpected higher mass than the prediction and higher rate of hadronic bottomonium transitions. The transition rate of $\Upsilon(5S) \to \pi\pi\Upsilon(nS)$ is about two orders of magnitude larger than those in $\Upsilon(1,2,3S)$ decays [1]. Meanwhile, the transition rate of $\Upsilon(5S) \to \pi\pi h_b$ is at the same order of magnitude despite this process requiring a b-quark spin-flip [2]. There are several hypothesis trying to explain these phenomena, for example, assuming the $\Upsilon(5S)$ consist of 4 four quarks in the wave function[3]. Another puzzle is the finding that the peak of $R_{\Upsilon(nS)\pi^+\pi^-} \equiv \sigma(\Upsilon(nS)\pi^+\pi^-)/\sigma^0_{\mu^+\mu^-}$ near $\Upsilon(5S)$ occurs at a mass 9 ± 4 MeV/c^2 higher than that derived from $R_b \equiv \sigma(b\bar{b})/\sigma^0_{\mu^+\mu^-}$ [4].

With a massive data around $\Upsilon(5S)$ collected at Belle detector based on KEKB collider, including 3 major points very near at $\Upsilon(5S)$ peak, 22 points with integrated luminosity of 1 fb^{-1} per point, and 61 points with integrated luminosity of 50 pb^{-1} per point, Belle collaboration is able to measure the Born cross sections around $\Upsilon(5S)$ and $\Upsilon(6S)$ region with improved precision.

2. $R_{\Upsilon(nS)}$ and R'_b measurements

Belle report the measurement of the total cross section for $e^+e^- \to \pi^+\pi^-\Upsilon(nS)$, $(n = 1,\ 2,\ 3)$ and $b\bar{b}$ quark pairs is based on all the datasets [5]. The distribution of $R_{\Upsilon(nS)\pi^+\pi^-}$, calculated using $N_{\Upsilon(nS)\pi^+\pi^-}/(\mathscr{L}_i\mathscr{B}(\Upsilon(nS) \to \mu^+\mu^-)\sigma^0_{\mu^+\mu^-}(\sqrt{s_i}))$, and the fit are shown in Fig. 1. A coherent sum of two S-wave Breit-Wigner amplitudes for $\Upsilon(5S)$ and $\Upsilon(6S)$ and a constant, plus an incoherent constant is used to fit the $R_{\Upsilon(nS)\pi^+\pi^-}$ distribution. The $\Upsilon(5S)$ and $\Upsilon(6S)$ masses, widths, and the relative phases are allowed to float. The fitting results are $M(\Upsilon(5S)) = (10891.1 \pm 3.2^{+0.6}_{-1.7})$ MeV/c^2, $\Gamma(\Upsilon(5S)) = (53.7^{+7.1+1.3}_{-5.6-5.4})$ MeV, $M(\Upsilon(6S)) = (10.987.5^{+6.4+9.0}_{-2.5-2.1})$ MeV/c^2, and $\Gamma(\Upsilon(6S)) = (61^{+9}_{-19}{}^{+2}_{-20})$ MeV.

The R'_b distribution, calculated using $R'_b \equiv R_{b,i} - \sum\sigma_{ISR,i}/\sigma^0_{\mu^+\mu^-,i}$, is shown in the bottom plot in Fig. 1. Note that the measurements yield the visible cross sections and include neither corrections due to the ISR events containing $b\bar{b}$ final states above $B\bar{B}$ threshold nor the vacuum polarization necessary to obtain the Born cross section. The background from the $q\bar{q}$, where $q = u,\ d,\ s,\ c$, are subtracted based on the data taken at 10.52 GeV with a scale of $1/s$, where $\sigma_{b\bar{b}} = 0$. With the same fitting method, the fit results are shown in Fig. 1. The fitting range is restricted to $10.82 - 11.05$ GeV to avoid complicated threshold effects below 10.8 GeV. A large resonance-continuum interference is reflected in this fit. Although the fitting results on resonance parameters are consistent with those from $R_{\Upsilon(ns)\pi^+\pi^-}$ fitting, the validity of using a flat continuum in the R'_b fit is brought into questions by incompatibilities between the fitted amplitudes for R'_b. and $R_{\Upsilon(nS)\pi^+\pi^-}$.

3. Energy Scan of $e^+e^- \to \pi^+\pi^-h_b(1,\ 2P)$ and evidence for charged bottomonium-like State

Belle also report the analysis on $e^+e^- \to \pi^+\pi^-h_b(1,\ 2P)$ using the full $\Upsilon(5S)$ and $\Upsilon(6S)$ scan data [6]. The measured Born cross section of $e^+e^- \to \pi^+\pi^-h_b(1,2P)$ are shown in Fig. 2. A simultaneous fit with coherent sum of two Breit-Wigner amplitudes is performed to the cross sections

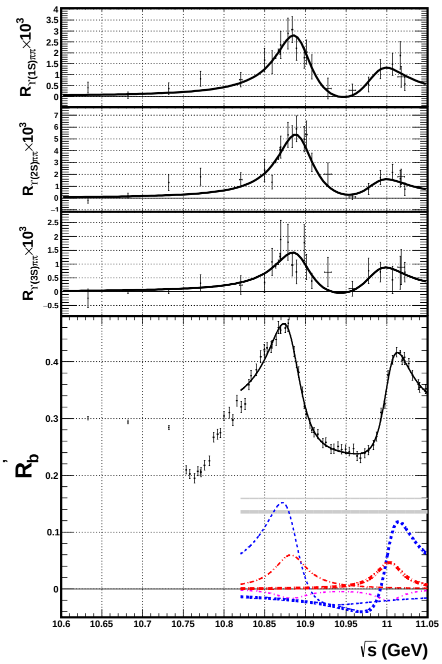

Figure 1: $R(\Upsilon(nS)\pi^+\pi^-)$ data with fit results for $\Upsilon(1S)$; $\Upsilon(2S)$; $\Upsilon(3S)$; and R'_b data with components of fit: $\Upsilon(5S)$ (thin) and $\Upsilon(6S)$ (thick).

and a continuum component is considered in the systematic uncertainty. The masses and widths of the measured resonances are $M = (10884.7^{+3.6+8.9}_{-3.4-1.0})$ MeV/c^2 and $\Gamma = (40.6^{+12.7+\ 1.1}_{-\ 8.0-19.1})$ MeV for $\Upsilon(5S)$; $M = (10999.0^{+7.3+16.9}_{-7.8-\ 1.0})$ MeV/c^2 and $\Gamma = (27^{+27+\ 5}_{-11-12})$ MeV for $\Upsilon(6S)$. The significances of $h_b(1P)$ and $h_b(2P)$ signals in the combined five data points around the $\Upsilon(6S)$ resonance are 3.5σ and 5.3σ, respectively. The intermediate resonant substructures from $\Upsilon(6S) \to \pi^+\pi^- h_b(1,2P)$ are checked via yielding h_b in bins of the recoiling mass of π. The distribution of the recoiling mass of π are shown in Fig. 2(a)(b) as well as the fitting function. The fitting results imply that the processes of $\Upsilon(6S) \to \pi^+\pi^- h_b(1,2P)$ are proceed entirely via the intermediate isovector $Z_b(10610)$ and $Z_b(10650)$. The hypothesis that only $Z_b(10610)$ is produced is excluded at the level of 3.3 standard deviations, while the hypothesis that only $Z_b(10650)$ is produced is not excluded at a significant level.

4. Study of $e^+e^- \to B_s^{(*)}\bar{B}_s^{(*)}$ Production

Belle also report the production of $e^+e^- \to B_s^{(*)}\bar{B}_s^{(*)}$ processes based on $\Upsilon(5S)$ on resonance data and the energy dependent cross section based on the scan data [7]. Clear signal of $e^+e^- \to \Upsilon(5S) \to B_s^{(*)}\bar{B}_s^{(*)}$ are observed, while no statistically significant signal of $e^+e^- \to \Upsilon(6S) \to B_s^{(*)}\bar{B}_s^{(*)}$ processes. The relative production rate of $B_s^*\bar{B}_s^*$, $B_s^*\bar{B}_s^{(*)}$, and $B_s\bar{B}_s$ final states at $\sqrt{s} = 10.866$ GeV, which is very close to the $\Upsilon(5S)$ peak, is measured to be $7 : 0.856 \pm 0.106(\text{stat.}) \pm 0.053(\text{syst.}) : 0.645 \pm 0.094(\text{stat.})^{+0.030}_{-0.033}(\text{syst.})$. An angular analysis of the $B_s^*\bar{B}_s^*$ final state produced at $\Upsilon(5S)$ peak is also

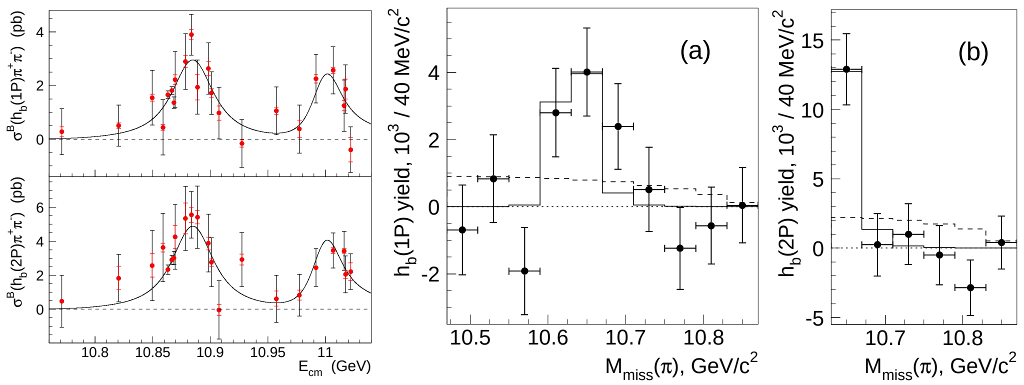

Figure 2: The cross sections for $e^+e^- \to h_b(1P)\pi^+\pi^-$ (left top) and $e^+e^- \to h_b(2P)\pi^+\pi^-$(left bottom) as function of center-of-mass energy, and the solid curves are the fit results. The efficiency corrected yields of $h_b(1p)\pi^+\pi^-$ (a) and $h_b(2P)\pi^+\pi^-$ (b) as functions of π recoiling mass for the combined data samples of five energy points in the $\Upsilon(6S)$ region, where points represent data, solid lines represent the fit results, and the dashed lines represent the fit results with a phase space distribution.

performed. The fraction of $S=0$ component is determined to be $r \equiv \frac{a_0^2}{a_2^2+a_0^2} = 0.175 \pm 0.057^{+0.022}_{-0.018}$. Energy dependent cross section of $e^+e^- \to B_s^{(*)}\bar{B}_s^{(*)}$ processes are shown in Fig. 3, which reveals a strong signal of $\Upsilon(5S)$ resonance while no significant signal of $\Upsilon(6S)$ resonance.

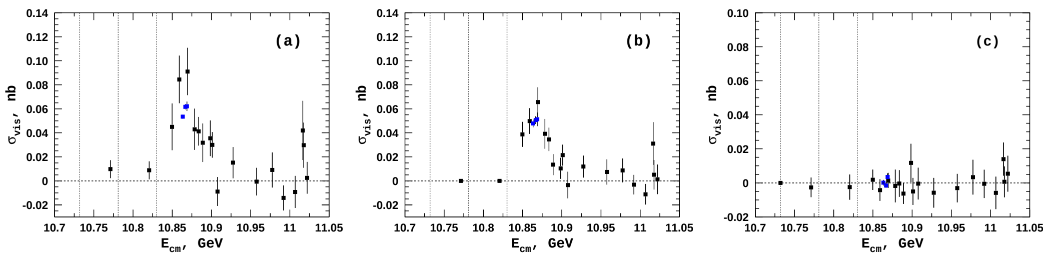

Figure 3: Cross section for the (a) total $e^+e^- \to B_s^{(*)}\bar{B}_s^{(*)}$; (b) $e^+e^- \to B_s^*\bar{B}_s^*$ only; (c) tagged B meson momentum sideband region. Vertical lines show the $B_s\bar{B}_s$, $B_s\bar{B}_s^*$, and $B_s^*\bar{B}_s^*$ thresholds, respectively.

5. Study of $e^+e^- \to \pi^+\pi^-\pi^0\chi_{bJ}$

The processes $e^+e^- \to \pi^+\pi^-\pi^0\chi_{bJ}$ are studied at $\sqrt{s} = 10.867$ GeV [8]. The $\gamma\Upsilon(1S)$ invariant mass distribution in the whole $\pi^+\pi^-\pi^0$ mass region after events selection is shown in Fig. 4 (left). Clear peaking signal of χ_{b1} and χ_{b2} are observed while χ_{b0} is not evident. An unbinned maximum likelihood fit is applied and the solid curve shows the fit results. The Born cross section of $e^+e^- \to \pi^+\pi^-\pi^0\chi_{bJ}$ are < 3.1 pb^{-1}, $= (0.90 \pm 0.11 \pm 0.13)$ pb^{-1}, and $= (0.57 \pm 0.13 \pm 0.08)$ pb^{-1} for $J = 0,\ 1$, and 2, respectively. Both $\omega\chi_{bJ}$ events and non-$\omega\chi_{bJ}$ events are observed in the $\pi^+\pi^-\pi^0$ mass spectrum. The mass spectra of $\gamma\Upsilon(1S)$ within and outside ω signal region are also shown in Fig. 4 (middle, right). The measured Born cross section $\sigma(e^+e^- \to \omega\chi_{bJ}) < 1.9$ pb^{-1}, $= (0.76 \pm 0.11 \pm$

0.11) pb^{-1}, and $= (0.19 \pm 0.11 \pm 0.08)$ pb^{-1} for $J = 0,\ 1$, and 2, respectively; while $\sigma(e^+e^- \to \pi^+\pi^-\pi^0_{\text{non}-\omega}\chi_{bJ}) < 2.3$ pb^{-1}, $= (0.25 \pm 0.07 \pm 0.06)$ pb^{-1}, and $= (0.30 \pm 0.11 \pm 0.14)$ pb^{-1}. This is the first observation of hadronic transitions between $\Upsilon(5S)$ and $\chi_{b1,2}$ bottomonium states. The measured ratio of the cross section of $e^+e^- \to \omega\chi_{b2}$ to $\omega\chi_{b1}$ is $0.38 \pm 0.16(\text{stat.}) \pm 0.09(\text{syst.})$, which is significantly lower than the expectation of 1.57 from the heavy quark symmetry.

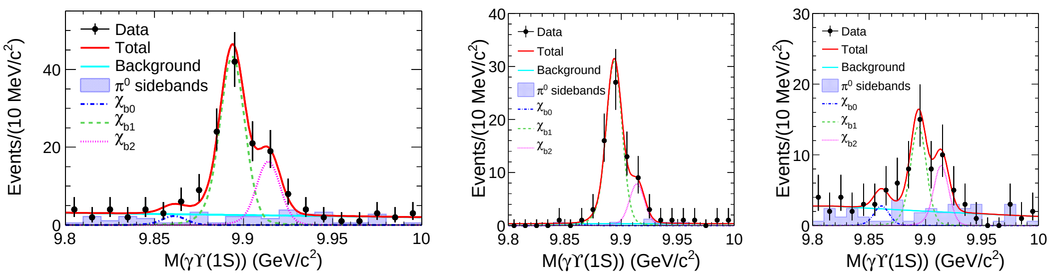

Figure 4: The $\gamma\Upsilon(1S)$ invariant mass distributions for selected $e^+e^- \to \pi^+\pi^-\pi^0\gamma\Upsilon(1S)$ candidate events in (left) whole $\pi^+\pi^-\pi^0$ mass regoin, (middle) the ω signal region, and (right) outside of ω signal region. The solid curves are the best fit for the total fit the background shape; the dash-dotted, dashed and dotted curves represent the χ_{b0}, χ_{b1}, and χ_{b2} signals, respectively.

6. Summary

The cross section measurements of $e^+e^- \to \Upsilon(nS)\pi^+\pi^-$, $b\bar{b}$, $\pi^+\pi^-h_b(nP)$, and $B_s^{(*)}\bar{B}_s^{(*)}$ between 10.63 and 11.02 GeV are performed and the resonance parameters of $\Upsilon(5S)$ and $\Upsilon(6S)$ mesons are obtained. It is interesting that the resonance peak of $\Upsilon(5S)$ from $B_s^{(*)}\bar{B}_s^{(*)}$ mode is different from those of $\Upsilon(nS)\pi^+\pi^-$ and $h_b(nP)\pi^+\pi^-$ modes, this is still a puzzle to us. The processes $\Upsilon(5S) \to \pi^+\pi^-\pi^0\chi_{b1,2}$ are observed for the first time.

References

[1] K. F. Chen *et al.* [Belle Collaboration], Phys. Rev. Lett. **100**, 112001 (2008).

[2] I. Adachi *et al.* [Belle Collaboration], Phys. Rev. Lett. **108**, 032001 (2012).

[3] A. Ali, C. Hambrock and M. J. Aslam, Phys. Rev. Lett. **104**, 162001 (2010) Erratum: [Phys. Rev. Lett. **107**, 049903 (2011)]/PhysRevLett.104.162001, 10.1103/PhysRevLett.107.049903.

[4] K.-F. Chen *et al.* [Belle Collaboration], Phys. Rev. D **82**, 091106 (2010).

[5] D. Santel *et al.* [Belle Collaboration], Phys. Rev. D **93**, no. 1, 011101 (2016).

[6] A. Abdesselam *et al.* [Belle Collaboration], Phys. Rev. Lett. **117**, no. 14, 142001 (2016).

[7] A. Abdesselam *et al.*, arXiv:1609.08749 [hep-ex].

[8] X. H. He *et al.* [Belle Collaboration], Phys. Rev. Lett. **113**, no. 14, 142001 (2014).